Low-energy pion scattering to 1^- states in ^{12}C

C. M. Kormanyos and R. J. Peterson
University of Colorado, Boulder, Colorado 80309

J. Applegate, J. Beck, T. D. Averett, and B. G. Ritchie
Department of Physics and Astronomy, Arizona State University, Tempe, Arizona 85287

C. L. Morris and J. McGill
H-841, Los Alamos National Laboratory, Los Alamos, New Mexico 87545

D. S. Oakley
Lewis and Clark College, Portland, Oregon 97219
(Received 18 December 1992)

Differential cross sections for 40, 50 and 65 MeV π^+ and π^- inelastic scattering to 1^- excitations in ^{12}C have been measured and compared to distorted wave impulse approximation (DWIA) reaction model predictions. Strengths are presented in terms of sum rules for the 1^- state at 10.84 MeV and for the giant dipole resonance from 18 to 25 MeV. An excitation function at q =224 MeV/c for the 1^- state at 10.84 MeV is displayed in the energy range from 50 to 291 MeV, showing a non-spin-flip pattern. We find inadequacies in the detailed comparison of the shapes of the data to DWIA calculations using several standard nuclear models.

PACS number(s): 25.80.Ek, 24.10.Ht

I. INTRODUCTION

Low pion beam energies emphasize transitions of low orbital angular momentum transfer L in inelastic scattering. Here we present data at 40, 50, and 65 MeV for pion scattering to known states of ^{12}C that require $L = 1$. With spin transfer $S = 0$ coupled to $L = 1$ we will examine states of ^{12}C with J^π of 1^-. At large scattering angles and low pion beam energies a very strong sensitivity to the isospin purity of inelastic transitions is known [1]. Therefore a comparison of π^+ to π^- data can determine sensitively the isospin purity of the transitions in ^{12}C, which are of special importance for 1^- excitations.

The 10.84 MeV 1^-; $T = 0$ state of ^{12}C [2] must be excited by an isoscalar electric dipole transition. This unusual mode is weakly excited since center-of-mass motion must be removed from the transition density that generates its scattering amplitudes. Collective models meeting the overall conditions are available to describe the 1^-;0 transitions [3, 4] but have never been compared to low-energy pion data. Data at low pion beam energies of 40, 50, and 65 MeV and the data for the 10.84 MeV 1^- state at higher beam energies [5] allow an excitation function at fixed three-momentum transfer q to cover a wide range of angle, going well beyond the obvious dominance of the 3-3 resonance. This allows a strong test of the role of spin transfer in pion scattering. Broad states related to the highly collective giant dipole resonance are found at higher excitations in ^{12}C, and their spin characteristics have been examined at higher beam energies and smaller angles [6]. Lower beam energies give a sensitive and different probe of these interpretations.

Measured cross sections to $L = 1$ transitions in ^{12}C will be compared to theoretical results of distorted wave impulse approximation (DWIA) calculations. Scattering from carbon at 40, 50, and 65 MeV has been very well measured, and has become the test case for optical model calculations. Thus the parameters are very well determined and have been taken from the literature [7].

II. EXPERIMENTAL METHODS

The experiment was performed at the Low Energy Pion (LEP) channel of the Clinton P. Anderson Meson Physics Facility (LAMPF). This experiment made use of a new superconducting energy compressor (SCRUNCHER) to increase the flux of low-energy pions with good resolution [8–10]. The beam spot for this beam line is achromatic with an energy resolution determined by momentum acceptance slits in the channel, which also limit the beam intensity. There is a strong correlation between the momentum and time of passage through this beam line that permits an external accelerating electromagnetic field within the SCRUNCHER to rotate the longitudinal phase space ellipse from wide beam slits to maintain good momentum resolution.

In the present work, the SCRUNCHER was located approximately 1.4 m upstream from the scattering target. In the cavity a voltage gradient of 2.37 MV/m was achieved at a frequency of 402.5 MHz, which is double that of the linear accelerator's 201.25 MHz frequency, with a Q of about 10^9. With momentum slits set for $\delta p/p = \pm 1.5\%$, the overall energy resolution was the same as our previous work [11] using the much less

intense pion beam available with a momentum bite of ±0.2%. Without the SCRUNCHER our resolution was 2 MeV, which improved to 700 keV [full width at half maximum (FWHM)] using the device. In the present work, the beam spot was oval shaped measuring approximately 4 cm wide by 2 cm high, which is nearly 2 times larger than the beam spot used during prior experiments on this line [11, 12]. To compensate for this change and to improve energy resolution of the spectrometer, a wire chamber was added in front of the spectrometer entrance. A solid graphite target of thickness 129.2 mg/cm^2 was used for the ^{12}C measurements.

We detected and analyzed scattered pions with the Clamshell spectrometer used for our previous studies on this beam line [11, 12]. The Clamshell solid angle is close to 40 msr. Measurements were made with positive pion beam energies of 40, 50, and 65 MeV and compared to π^- spectra at several angles at 50 and 65 MeV. The maximum laboratory scattering angle was 103°.

The momentum acceptance of the spectrometer system was measured by sweeping the π^+-p elastic peak (from a 274.8 mg/cm^2 CH_2 target) across the focal plane detectors. Scattered pions were identified using a time-of-flight measurement after the scattering target and a total energy measurement at the spectrometer focal plane. The primary proton production current at LAMPF, which is proportional to the pion flux in the LEP channel, was monitored with torroid and ion chamber monitors. However, each inelastic carbon spectrum was normalized to previous results for elastic and strong inelastic pion scattering [13–16]. Excitation energies in the carbon spectra were calibrated internally using the known excitation energies of several strong peaks [2]. The uncertainty in the resulting energy calibration was ±140 keV.

The width of the acceptance was 45% between half maxima, and the spectrometer was set such that the central ray was associated with a 12 MeV excitation in ^{12}C. This wide spectrum gave a clear giant dipole resonance (GDR) peak at the 50 MeV beam energy, but this is not included in the present results due to insecurities at the edges of the acceptance. At 65 MeV we have good data for the GDR region from 20 to 25 MeV in excitation energy, as shown in Fig. 1.

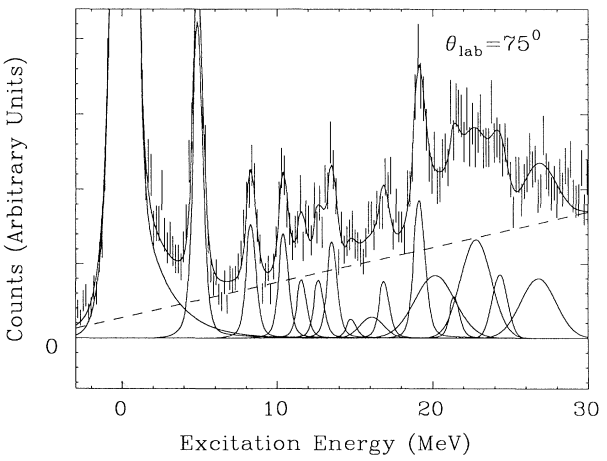

FIG. 1. A fitted spectrum of 65 MeV π^+ from ^{12}C at 75° is shown. The dashes are the acceptance corrected data with the solid line fit drawn through, including only known states. The components of the GDR from 20 to 25 MeV are discussed in Sec. IV B. The dashed line shows the background. Peaks with the background subtracted are indicated. Only statistical uncertainty is included.

Peak fitting for determination of differential cross sections of inelastic transitions of known intrinsic widths less than the experimental resolution used a Gaussian peak shape folded with three exponential tails which had been fit to the shape of the elastic peak. Wider peaks were fit with Gaussian peak shapes of variable width. Simultaneously a polynomial background up to order 2 was drawn below known peaks. The spectrum of Fig. 1 shows an example of the peak fitting. Uncertainties quoted for the cross sections are the statistical uncertainties from peak fitting and do not include any uncertainty in the overall normalization, estimated to be ±10%.

III. REACTION MODELS

All DWIA calculations were carried out with the code DWPIES [17]. The ground state density distribution used for ^{12}C was a shperically symmetric three-parameter Fermi (3PF) shape,

$$\rho(r) = \frac{\rho_0[1 + w(r/c)^2]}{1 + \exp[(r-c)/z]}, \quad (1)$$

with parameters fitted to the known charge density in Ref. [18] giving (2.384,0.452,−0.100) fm for (c, z, w). First-order optical model parameters were evaluated from the solutions of Rowe, Solomon, and Landau [19], while the second-order parameters were adjusted to match the elastic cross sections at each beam energy in published work.

The isoscalar electric dipole (ID) transition density of Ref. [3] was used for the $1^-;0$ excitaton at 10.84 MeV. The transition density (neglecting small terms) is

$$\rho_{tr}(r) = -\frac{\beta_1}{c\sqrt{3}}\left[3r^2\frac{d}{dr} + 10r - \frac{5}{3}\langle r^2\rangle\frac{d}{dr}\right]\rho_0(r), \quad (2)$$

where

$$\beta_1^2 = \frac{6\pi\hbar^2}{mAE_x}c^2/(11\langle r^4\rangle - \tfrac{25}{3}\langle r^2\rangle^2), \quad (3)$$

with β_1 chosen to exhaust the isoscalar dipole energy weighted sum rule and c the half-density radius of the ground state matter distribution $\rho_0(r)$. The ID transition density times r must integrate to zero over all radii to prevent motion of the nuclear center of mass. This transition density has a node, in contrast to the case of the usual collective model for surface vibrations which uses the derivative of the ground state density. Because of the transparency of nuclei to low-energy pions, this node has an important effect on the calculated cross sections.

Nonspin excitations of the $T = 1$ GDR peak from 20 to 25 MeV have been modeled in the impulse approximation even though the pion energy loss is around half of

the initial beam energies used. To investigate the role of the nuclear transition densities for this $1^-;1$ transition, we have used the Goldhaber-Teller (GT) and Steinwedel-Jensen (SJ) models for antisymmetric oscillations of neutrons and protons. In the GT model, the transition density is given by

$$\rho_{\rm tr}(r) = -\beta_{\rm GT} c \frac{d}{dr}\rho_0(r), \tag{4}$$

with

$$(\beta_{\rm GT} c)^2 = 4\pi \left(\frac{\hbar^2/2m}{\hbar\omega}\right) \frac{N}{AZ} = 1.006\,{\rm fm}^2; \tag{5}$$

to exhaust 100% of the usual photoelectric sum rule with the ground state 3PF form for $\rho_0(r)$.

For the SJ model, the transition density of Ref. [20] was used:

$$\rho_{\rm tr}(r) = \beta_{\rm SJ}\, \rho_0(r)\, j_1(2.08r/c). \tag{6}$$

Here

$$\beta_{\rm SJ}^2 = 4\pi \left(\frac{\hbar^2/2m}{\hbar\omega}\right) \frac{N}{AZ} \frac{9}{I^2} = 12.50, \tag{7}$$

to exhaust the dipole sum rule, and the normalizing radial integral is

$$I = \int_0^\infty \rho_0(r)\, j_1(2.08r/c) r^3 dr = 0.8509\,{\rm fm} \tag{8}$$

for ^{12}C. Figure 2 shows the dipole form factors used in the present work. Results for the GDR strengths will be compared to those that exhaust 100% of these sum rule strengths.

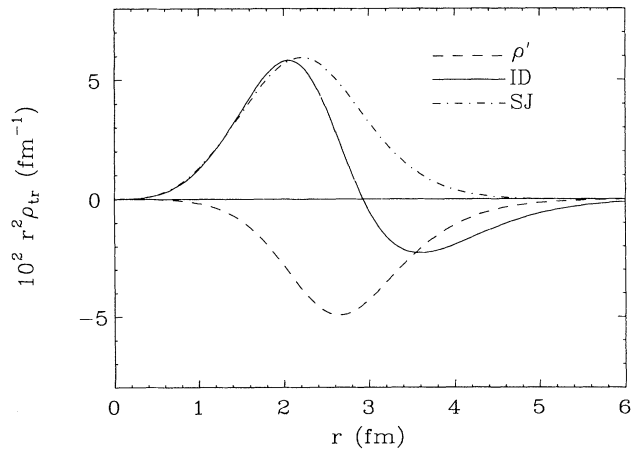

FIG. 2. Several dipole transition densities used for DWIA calculations in the present work are shown. The solid line corresponds to the isoscalar electric dipole transition density, appropriate for the $1^-;0$ state at 10.84 MeV. The dot-dashed line shows the SJ transition density used for the GDR calculations. The dashed line shows the derivative of the ground state density used for collective model calculations of both the GDR and the 10.84 MeV states. The phase convention for the three curves was chosen for clarity of the picture, while the calculations used the phases documented in the text.

IV. RESULTS

Several well-known $L = 0$ states were analyzed for consistency. Cross sections were determined for the 0^+ state at 7.65 MeV, without spin flip, and the 1^+ states of isospin 0 at 12.71 MeV and isospin 1 at 15.11 MeV. The 0^+ cross sections at 65 MeV were found to agree well with the 67.5 MeV data compared to the theoretical calculations in Ref. [7]. Our confirmation of a dropping cross section at forward angles contrasts to theoretical results which insist on rising at forward angles. The spin flip 1^+ transitions at 50 MeV agree with earlier results for the 12.71 MeV peak [12], and both π^+ and π^- data at 50 MeV are found to agree with the published results of Jaki *et al.* [21]. The data for the strong low-energy, low-spin excitations are presented in Ref. [10].

A. $1^-;0$ state at 10.84 MeV

Differential cross sections for π^+ excitation of the known $1^-;0$ state at 10.84 MeV with a width of 315 ± 25 keV [2], smaller than the experimental resolution, are shown in Fig. 3 at three beam energies. Complementary π^- data at 50 MeV and 65 MeV show the consistency expected by charge symmetry. Charge symmetry for this transition has also been demonstrated at 180 MeV [22], using the Energetic Pion Channel and Spectrometer (EPICS) system at LAMPF. The connection between charge symmetry and the strength of such an isoscalar dipole transition has been pointed out by Millener [23].

Solid curves compared to the data in Fig. 3 were computed with the ID transition density and an isoscalar

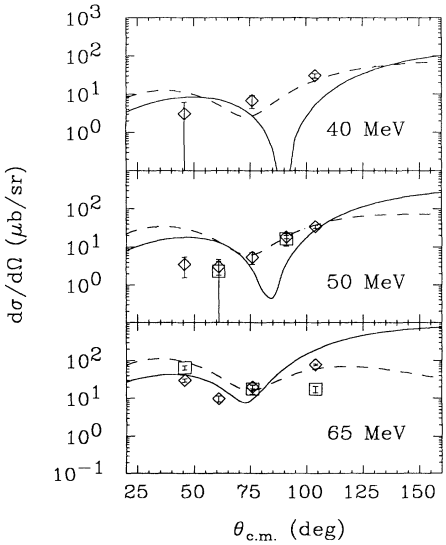

FIG. 3. DWIA calculations using the isoscalar transition density in solid are compared to dashed lines computed using a derivative collective model transition density. Data and calculations for π^+ (diamonds) at energies of 40 MeV, 50 MeV, and 65 MeV are shown for the 10.84 MeV $1^-;0$ state of ^{12}C. Complementary π^- data at 50 MeV and 65 MeV are shown as squares, confirming approximate charge independence for this particular interaction.

π-A interaction. The dashed curve was computed using the derivative of the ground state density for the transition density—a surface vibrational mode that does not preserve the motion of the nuclear center of mass. The magnitudes of the theory curves shown in Fig. 3 were adjusted to yield an overall fit to the data. The corresponding fraction of the isoscalar dipole energy weighted sum rule exhausted by this one state is 3.1% for both the ID model and the derivative model for all three low-energy pion beam energies. The ID transition density calculations feature a deep minimum not shown by the data. Evidently the derivative model more closely resembles the true transition density in the radial region that generates low-energy pion scattering to this state.

Data for π^+ scattering at higher energies were taken and analyzed during the work of Ref. [22] but not published. We take the opportunity to present these differential cross sections at 180 MeV in Fig. 4 compared to calculations using both the isoscalar and derivative transition densities. At this higher energy, the scattering is highly diffractive. The two calculations are out of phase with one another, and the isoscalar model seems to match the shape of the data better. Again, 3.1% of the sum rule strength is observed for 180 MeV π^+ scattering to this state.

At 180 MeV, the $1^-;0$ differential cross section peaks at a three-momentum transfer of 224 MeV/c. Figure 5 shows differential cross sections from 50 to 291 MeV for this fixed q. At 40 MeV there is no kinematical solution with q =224 MeV/c, and at 50 MeV and 80 MeV an extrapolation from the ID theory curve was used to estimate the cross section. The dotted line in Fig. 5 is proportional to the $\cos^2\theta$ expectation for the trend of a nonspin pion transition [24]. Also shown in Fig. 5 are the DWIA excitation functions for both the ID and derivative form factors. This excitation function shows a clean, nonspin reaction mode and the comparison of π^+ and π^- data shows a cleanly isoscalar mode. Inelastic electron scattering to the isoscalar 1^- state at 7.12 MeV in ^{16}O has been analyzed in terms of the mixing of a small T=1 component in the nuclear level [25]. This would tend to spoil the charge symmetry seen here for π^+ and π^-.

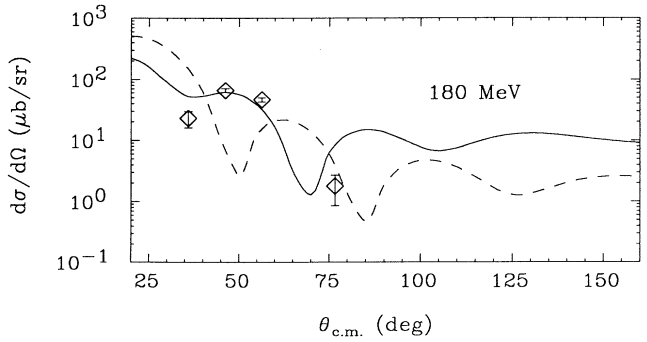

FIG. 4. Data and DWIA calculations for π^+ at 180 MeV are shown for the 10.84 MeV $1^-;0$ state of ^{12}C. The calculation using the isoscalar transition density is shown in solid compared to the dashed line computed using a derivative collective model transition density.

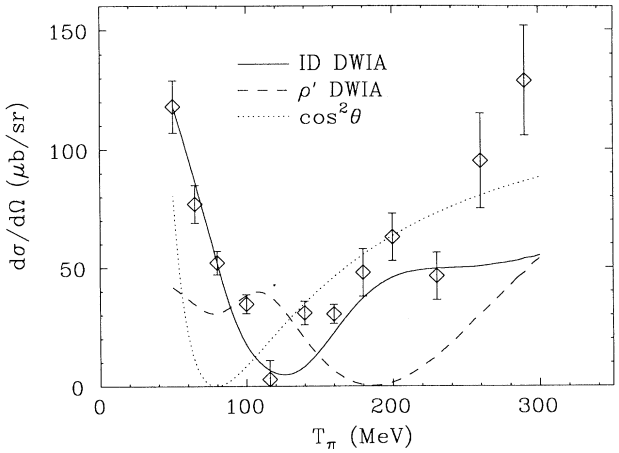

FIG. 5. Fixed momentum transfer excitation function at q =224 MeV/c for the $1^-;0$ state at 10.84 MeV in ^{12}C is shown for positive pion energies between 50 and 291 MeV. The dotted line is proportional to $\cos^2\theta$. The dashed line was computed using the derivative collective model transition density, while the solid line was computed with the isoscalar transition density of Ref. [3]. The trend of a nonspin pion excitation is clearly visible.

Other pion excitations of 1^- states in light nuclei also are found not to agree with optical model calculations. The resonance pion data of Geesaman *et al.* [26] from the 1^+ ground state of ^{14}N to 0^- and 1^- final states are directly out of phase with the DWIA calculations using the derivative transition density, as found here, and also call for comparison to the ID transition density.

The collectivity of the $1^-;0$ example in ^{12}C at 10.84 MeV is important because of the relation to nuclear compressibility. While 0^+ to 0^+ transitions correspond to collective breathing modes, the dipole collective mode corresponds to compression and dilation along a specific axis [27]. In a harmonic oscillator model all $1\hbar\omega$ motion is spurious, and only $3\hbar\omega$ amplitudes contribute. Many-body random phase approximation (RPA) calculations for heavier nuclei have predicted a collective $1^-;0$ mode near $150/A^{1/3}$ MeV [27], corresponding to 65 MeV in ^{12}C, with transition densities much like the collective ID model used here. Significant electric dipole strength at only 10.84 MeV in ^{12}C is thus surely of general interest.

B. GDR

The photonuclear GDR in ^{12}C is comprised of several components between 18 and 25 MeV. In Fig. 6 our 65 MeV spectrum at 75° is compared with a (γ, n) spectrum from Ref. [28], showing a similarity but not the same detailed features. Also in Fig. 6 we show the GDR region of ^{12}C excited by resonance energy pions [6]. In each of the three spectra shown, the most significant strength is around 23 MeV with a smaller, distinct peak near 25 MeV. In addition, in the two-pion spectra one can discern

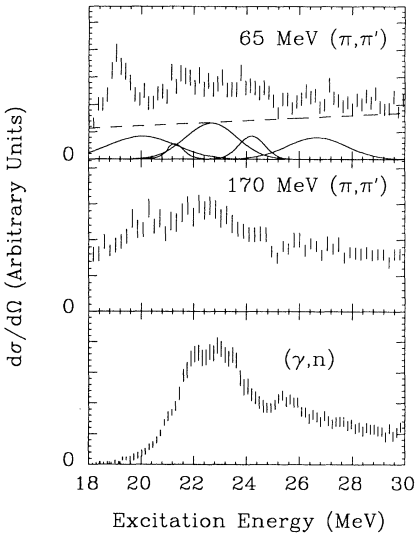

FIG. 6. Acceptance-corrected spectrum of 65 MeV π^+ at a laboratory scattering angle of 75°, with the dashed line background and solid line fitted peaks shown, is compared with a spectrum from Ref. [6] excited by 170 MeV positive pions at 22° and with a (γ, n) spectrum of Ref. [28] in the GDR region. All three spectra are for ^{12}C and feature similar components.

other, smaller peaks. We have followed the same fitting scheme used in Ref. [6] to decompose our GDR peak into consistent components, as listed in Table I. An example showing these GDR pieces above a background for 65 MeV positive pions at a laboratory scattering angle of 75° is shown in Fig. 6. All the GDR pieces have angular distributions similar to the strongest peak, which is the third component at 23 MeV.

We have carried out DWIA calculations in the isovector channel for both the GT and SJ models. The node in the nuclear surface in the SJ model should give different predictions from the GT model at low pion energies for which the projectile mean free path is great enough to be influenced by features at smaller radii. Data and calculations are displayed in Fig. 7. The magnitudes of all the DWIA calculations for the GDR pieces were determined by forcing the theory curve to overlap with the π^+ data

TABLE I. Centroids and widths for the discrete peaks fit to the GDR region for ^{12}C, as shown in Fig. 1 for 65 MeV π^+ at 75°. These values are those obtained for resonance energy pion scattering in Ref. [6]. Also are shown the maximum c.m. differential cross section and the sum rule fraction (SRF) observed for each GDR piece calculated using the SJ model.

E_x in ^{12}C (MeV)	Γ (keV)	$\frac{d\sigma}{d\Omega}$ (μb/sr)	SRF (%)
19.85	330	122	15.3
22.10	198	14	3.1
22.94	192	168	18.8
23.70	79	42	6.3
25.40	232	128	14.7

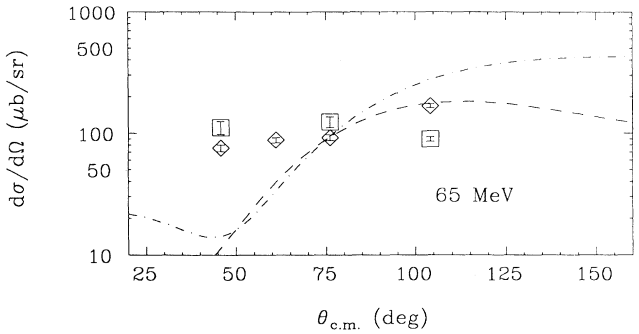

FIG. 7. DWIA calculations for 65 MeV π^+ (diamonds) and π^- (squares) scattering from ^{12}C are compared to the third, most prominent peak, in the GDR data. The dashed line uses the GT model, the dot-dashed line uses the SJ model.

point at a laboratory scattering angle of 75°. For the GT model 31% of the sum rule strength is exhausted for the strongest GDR component at 23 MeV, compared with 19% for the SJ model. Also shown in Fig. 7 are 65 MeV π^- GDR data; charge symmetry between π^+ and π^- is exhibited to within about 30%. The SJ model gives an angular distribution similar to the GT model since the radius of ^{12}C is comparable to the radius of the first node in the SJ transition density. Neither the GT nor the SJ model has success in matching the data. For the GT model the sum of all the fitted GDR pieces accounts for 95% of the sum rule discussed in Sec. IV B, compared with 58% for the SJ model with the same cross sections.

V. CONCLUSIONS

We have measured π^+ and π^- inelastic scattering cross sections to known 1^- states of ^{12}C, using the SCRUNCHER to achieve the flux needed to observe the $1^-;0$ state at 10.84 MeV. No pion data and few other results are available for this transition, which is of interest because the most obvious reaction models are not permitted for it. We used low-energy pions, with a mean free path suggesting access beyond the surface of the target nucleus, to improve the sensitivity to the nuclear models. The expected charge symmetry is observed for π^+ and π^- cross sections. Use of the ID transition density reaction model, which does conserve the motion of the center of mass, gave DWIA predictions in poorer agreement with the data than did use of the incorrect derivative vibrational model at these energies. At resonance, the diffraction pattern was better reproduced with the ID model, which should be superior. The fixed three-momentum transfer excitation function, from 50 MeV to 291 MeV, was matched better by DWIA calculations using the ID model and indicated a nonspin ($S = 0$) pattern. The strength, expressed as a fraction of a sum rule, is approximately constant throughout the range of beam energies considered.

The large acceptance of the Clamshell spectrometer also permitted data at 65 MeV at the same time for the isovector GDR, best known from photonuclear stud-

ies. Comparison to the (γ, n) and resonance-energy pion spectra shows similar characteristics of these excitations of the GDR near 23 MeV. The present data exhibit charge symmetry between π^+ and π^- to about 30%. The strongest portion of this broad peak, fit using spectroscopic parameters found by resonance pion scattering, gave an angular distribution that was reproduced by neither of the two popular collective models for the GDR. Less than 50% of the energy weighted sum rule was exhausted by this portion of the peak, while the sum of all fitted portions of the GDR exhausted 95% of the GT sum rule compared with 58% of the SJ sum. Low-energy pions should be more sensitive to subtle features of the nuclear transition densities by better access to the nuclear interior. The inadequacies found in the detailed comparison to DWIA calculations of several standard nuclear models point up a problem with either these models or with the use of the DWIA for the two states described here.

ACKNOWLEDGMENTS

This research was supported in part with funds granted by the National Science Foundation and in part by the U.S. Department of Energy under Contract No. DE-FG02-86ER40269. Also we would like to acknowledge W. B. Cottingame for permission to use his previous work and the scientists and staff at LAMPF for their greatly appreciated assistance.

[1] R. Tacik, K. L. Erdman, R. R. Johnson, and H. W. Roser, Phys. Rev. Lett. **52**, 1276 (1984).
[2] F. Azjenberg-Selove, Nucl. Phys. **A333**, 1 (1985).
[3] M. N. Harakeh and A. E. S. Dieperink, Phys. Rev. C **23**, 2329 (1981).
[4] G. Orlandini, S. Stringari, and M. Traini, Phys. Lett. **119B**, 21 (1982).
[5] W. B. Cottingame (private communication).
[6] L. C. Bland, Ph.D. dissertation, University of Pennsylvania (1984); LANL Report No. LA-9960-T, 1984.
[7] R. Alvarez del Castillo and N. B. deTakacsy, Phys. Rev. C **43**, 1389 (1991).
[8] J. M. O'Donnell *et al.*, Nucl. Instrum. Methods A **317**, 445 (1992).
[9] J. D. Zumbro, H. A. Thiessen, C. L. Morris, and J. A. McGill, Nucl. Instrum. Methods B **40/41**, 896 (1989).
[10] J. M. Applegate, M. S. thesis, Arizona State University, 1992.
[11] B. G. Ritchie *et al.*, Phys. Rev. C **41**, 1668 (1990).
[12] B. G. Ritchie *et al.*, Phys. Rev. C **37**, 1347 (1988).
[13] M. Blecher *et al.*, Phys. Rev. C **20**, 1884 (1979).
[14] B. M. Preedom *et al.*, Phys. Rev. C **23**, 1134 (1981).
[15] R. J. Sobie *et al.*, Phys. Rev. C **30**, 1612 (1984).
[16] M. Blecher *et al.*, Phys. Rev. C **28**, 2033 (1983).
[17] E. R. Siciliano, computer code DWPIES, based on the code DWPI, R. A. Eisenstein and G. A. Miller, Comput. Phys. Commun. **11**, 95 (1976).
[18] H. deVries, C. W. deJager, and C. deVries, At. Data Nucl. Data Tables **36**, 495 (1987).
[19] G. Rowe, M. Salomon, and R. H. Landau, Phys. Rev. C **18**, 584 (1978).
[20] J. Speth and A. van der Woude, Rep. Prog. Phys. **44**, 46 (1981).
[21] J. Jaki *et al.*, Phys. Lett. B **238**, 36 (1990).
[22] W. B. Cottingame *et al.*, Phys. Rev. C **36**, 230 (1987).
[23] D. J. Millener, Phys. Rev. C **22**, 1355 (1980).
[24] E. R. Siciliano and G. Walker, Phys. Rev. C **23**, 2661 (1981).
[25] H. Miska, H. D. Graf, A. Richter, D. Schull, E. Spamer, and O. Titze, Phys. Lett. **59B**, 441 (1975).
[26] D. F. Geesaman *et al.*, Phys. Rev. C **27**, 1134 (1983).
[27] N. Van Giai and H. Sagawa, Nucl. Phys. **A371**, 1 (1981).
[28] B. L. Berman and S. C. Fultz, Rev. Mod. Phys. **47**, 713 (1975).